INTERROGATING A THIN LAYER OF HETEROGENEITY WITH CONFOCAL TRANSDUCERS

John G. Harris
Theoretical and Applied Mechanics, UIUC
216 Talbot Laboratory, 104 South Wright Street
Urbana, IL 61801

Douglas A. Rebinsky
Mechanical and Aerospace Engineering
Rutgers University
Piscataway, NJ 08855

Gerry Wickham
Department of Mathematics
Brunel University
Uxbridge, England, UK

INTRODUCTION

This is an expository summary of our work [1] building a mathematical model of scanned acoustic imaging of complicated solid-solid interfaces comprised of scatterers at several length scales, many of which are less than a wavelength. We construct an approximate two dimensional model of a scanned confocal acoustic imaging arrangement operating in a transmission or reflection mode using anti-plane shear or SH waves. Further, we suggest how the sound scattered from the interface is mapped into the sound collected by the transducers. The scalar approximation, while restrictive, still captures many of the basic ideas, ideas that we are at present extending to a three dimensional calculation.

The work that served to motivate this study is that of Margetan et al. [2]. They constructed model, solid-solid interfaces and interrogated them with compressional waves, reporting their experimental results as generalized transmission and reflection coefficients. They defined each coefficient, at a given frequency, as the temporal Fourier component of the signal transmitted by or reflected from the interface divided by the temporal Fourier component of a reference signal. Either a single focused transducer or focused transducers arranged as a coaxial confocal pair were used to direct ultrasound across a layer of fluid

Review of Progress in Quantitative Nondestructive Evaluation, Vol. 15
Edited by D.O. Thompson and D.E. Chimenti, Plenum Press, New York, 1996

couplant and into the solid specimen, with approximate focusing taking place at the mean plane of the interface.

Although imperfections may occur at many length scales, Margetan et al. [2] were principally concerned with those whose lengths varied between 100 and 1000 μm. They operated their transducers at frequencies in a neighborhood of 5 to 10 MHz. Because the transducer apertures were many wavelengths in diameter and the focal regions large enough to encompass more than one scatterer, at each scan position, the signals scattered from several heterogeneities in the interface, along with signals resulting from multiple scattering among the heterogeneities, were all collected. Recall that each transducer's voltage is the summed magnitude and phase of all these signals. Accordingly, the generalized transmission and reflection coefficients measured, at each point along the interface were the outcome of complex multiple scattering events.

THEORY

Here we give a summary of the model. A complete discussion, along with a discussion of related research by others is given in [1]. The model is a combination of a theory of scattering from thin interfaces, plates or shells advanced by Wickham [3], and a model advanced by Yogeswaren and Harris [4] of how the scattered sound is collected by the receiving transducers.

Model of the Heteogeneous Layer

Our purpose is to examine the reflection from and transmission through a general interface insonified by a focused beam. Figure 1 shows the geometrical configuration we have in mind. We introduce three approximations to enable us to do this.

Firstly, we consider the anti-plane shear problem rather than the fully three-dimensional one, anticipating that many of the general features will not be lost with this approximation.

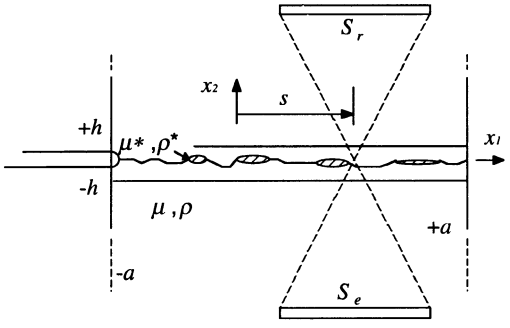

Figure 1. The geometrical configuration of a typical interface to be interrogated and of the focused beam scanning the interface.

Secondly, we embed the interface to be interrogated within a large cell, width $2a$, that is periodically repeated. Within each cell scatterers at many smaller variations in characteristic size are enclosed. These scatterers may have different mechanical properties and the geometry of the interface may vary. Figure 1 shows inclusions with shear constant μ^* and density ρ^*. The upper and lower interfaces are indicated by η^+ and η^-, respectively. The whole interface is enclosed within a layer of thickness $2h$. Because the interrogating beam is focused, we anticipate a localized interaction over a region small compared with the length scale a along the interface (the x_1 direction). This strategy is a mathematical device that effectively truncates the domain of integration of the partial differential equations to an infinite strip of finite width.

Thirdly, we characterize the interface by its polarizations, namely,

$$\sigma_{\beta 3} = (\mu^* - \mu)\partial_\beta u_3 \quad \text{and} \quad p_3 = \omega(\rho^* - \rho)u_3. \tag{1a, b}$$

We are concerned with interfaces where the dimensionless parameter $(kh) < 1$ (k is the wave number). Provided the material contrasts

$$M^* = (\mu^*/\mu - 1) \quad \text{and} \quad D^* = (\rho^*/\rho - 1) \tag{2a, b}$$

are not too great the average polarizations are $O(kh)$. The Green's terms that appear in the integral representation may then be approximately evaluated on the mean plane and the polarizations averaged through the thickness so that the scattered wave field is represented by an integration over a plane rather than a volume. The outcome of these approximations is the following representation for the total wave field.

$$u_3(\vec{y}) = u_3^i(\vec{y}) - \frac{h}{\mu}\int_{-a}^{a}[\hat{\sigma}_{\beta 3}(x_1)\partial_\beta u_3^g(x_1, \vec{y}) - \omega u_3^g(x_1, \vec{y})\hat{p}_3(x_1)]dx_1 \tag{3}$$

where

$$\hat{\sigma}_{\beta 3} = \frac{1}{h}\int_{-h\eta^-}^{h\eta^+}\sigma_{\beta 3}dx_2 \quad \text{and} \quad \hat{p}_3 = \frac{1}{h}\int_{-h\eta^-}^{h\eta^+}p_3 dx_2\,. \tag{4a,b}$$

The upper and lower boundaries, controlling the degree of contact of the interface, are described by $x_2 = h\eta^{\pm}(x_1/a)$. The Green's function is given by Eqs. (7) through (10) of [1]. Expanding the average polarizations as Fourier series

$$\hat{\sigma}_{\beta 3} = \mu\sum_{q=-\infty}^{\infty}\xi_{\beta q}\, e^{iq\pi x_1/a} \quad \text{and} \quad -\hat{p}_3 = \rho c\sum_{q=-\infty}^{\infty}\xi_{3q}\, e^{iq\pi x_1/a} \tag{5a,b}$$

(c is the wave speed of the host material) reduces Eq.(3) to

$$u_3(\vec{y}) = u_3^i(\vec{y}) - \frac{h}{2}\sum_{n=-\infty}^{\infty}\frac{1}{\kappa_n}[\xi_n + \kappa_n \operatorname{sgn}(y_2)\xi_{2n}]\, e^{ik[(n\pi/ka)y_1 + \kappa_n|y_2|]} \tag{6}$$

where

$$\xi_n = (n\pi/ka)\xi_{1n} + i\xi_{3n} \quad \text{and} \quad \kappa_n = [1-(n\pi/ka)^2]^{1/2} \tag{7a,b}$$

and $sgn(x)$ denotes the distribution $[2H(x)-1]$. An infinite system of algebraic equations for the unknown Fourier coefficients ξ_n and ξ_{2n} is constructed by forcing self-consistency on Eq.(6).

Measurement Model

We now introduce definitions of the generalized reflection and transmission coefficients. The suggested definitions model the fact that a transducer integrates all the scattered waves striking its aperture to produce a voltage, but that, among those waves, the dominant contributions come from those that phase match to the incident wave. The incident wave field is a focused beam whose construction is described in [1] and is essentially identical to that used in [5].

To define generalized transmission and reflection coefficients we begin by applying a reciprocity relation to a region bounded by the receiving aperture S_r and the emitting aperture S_e, and containing the interface. One of the reciprocating wave fields is the incident wave field plus that scattered from the interface, while the other is selected so as to provide an integrated measure of the responses at one or the other of the transducer apertures [1]. The outcome of these arguments is the following definition of the generalized transmission coefficient $\overline{T}$, with a similar one for the generalized reflection coefficient $\overline{R}$.

$$\overline{T} = \frac{1}{P}\int_{-\theta_b}^{\theta_b} T_r(\theta)\cos^2\theta\, E^*(\sin\theta)\, E(\sin\theta)\, d\theta. \tag{8}$$

The coefficient $T_r(\theta)$ is a measure of the scattered wave field at a single point on the aperture S_r and $2\theta_b$ measures the angular extent of the aperture. The constant P is a normalization that makes $\overline{T}$ one when T_r is one . The function $E(x)$ models the shading of the aperture. It is given by

$$E(x) = [U_3/(2ka\kappa)]\, e^{-(Fx/\kappa)^{2m}} \tag{9}$$

where F and m are parameters controlling the shape of the beam, and U_3 is a constant. The * indicates the complex conjugate. Finally, using the reciprocity relation and Eq.(3), we obtain an expression for the generalized transmission coefficient $\overline{T}$ in terms of the Fourier coefficients of the interfacial polarizations, namely,

$$\overline{T} - 1 = \frac{-h\pi}{2ka\,P}\sum_{n=-N}^{N} E^*(n\pi/ka)\, e^{in\pi s/a}\,(\xi_n + \kappa_n\xi_{2n}). \tag{10}$$

Similar arguments give the generalized reflection coefficient $\overline{R}$ as

$$\overline{R} = \frac{-h\pi}{2ka\,P} \sum_{n=-N}^{N} E^*(n\pi/ka)\, e^{in\pi s/a}\, (\xi_n - \kappa_n \xi_{2n}). \tag{11}$$

NUMERICAL EXPERIMENTS

In [1] we show several plots of the change in transmission $|1-\overline{T}|$ for model interfaces. In the following numerical experiments we explore the difference between $\overline{T}$ and $\overline{R}$. In the limit of an open crack with traction free surfaces we should expect $\overline{R} = 1-\overline{T}$, while in the limit of a rigid layer we should expect $\overline{R} = \overline{T} - 1$.

Figure 2 shows the interface we explore here. The distance $ka = 26.7$ and corresponds approximately to 7.5 mm in water at 1 MHz. The ratio $kh/ka = 0.019$. Reference to Fig.3 of [1] would show that the focal region occupies approximately 40 scan units so that 3 cylinders are insonified at each position. We consider three material combinations: gold inclusions in glass, $M^* = -0.014$ and $D^* = 6.70$; gold inclusions in lucite, $M^* = 19.0$ and $D^* = 15.0$; yttria inclusions in IN100, $M^* = -0.230$ and $D^* = -0.360$. The case with gold in glass somewhat larger material contrasts than our theory was designed for, but does give a good contrast in the shear constants.

In Figures 3 to 5 we plot $|\overline{R}|$, the solid line, and $|1-\overline{T}|$, the dashed line, with cylinders ± 1 and ± 4 removed, over half the cell (the interface is symmetric). In each case the absent cylinders are clearly indicated, but only for the yttria in IN100 is there a strong difference between what is reflected and what is transmitted.

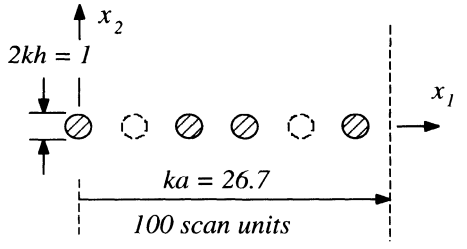

Figure 2. Half an interface comprised of symmetrically arranged, small penetrable cylinders that can be removed at will. The cylinders are numbered from 0 to 5, with cylinder 0 being at the origin. The dashed cylinders indicate those removed.

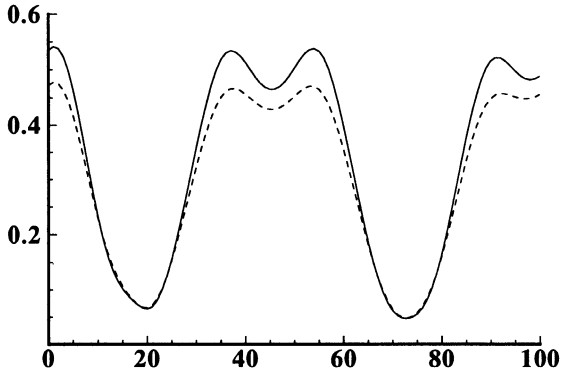

Figure 3. $|\overline{R}|$, the solid line, and $|1-\overline{T}|$, the dashed line, are plotted over half the cell for gold inclusions in lucite. Cylinders ±1 and ±4 have been removed.

CLOSURE

The model is founded on three ideas. Firstly, the sources of the scatter may be accurately represented by the through-thickness mean stress and momentum polarizations. Secondly, the response of a focused transducer or a coaxial confocal pair of transducers may be represented in terms of certain well defined generalized transmission and reflection coefficients. These coefficients take account of the fact that, while many signals are collected by its aperture, essentially the transducer acts reciprocally and responds most strongly to the signals that phase match with the emitted signal. Thirdly, the mathematical device of introducing a large scale, periodic structure can be used to effectively truncate the ideally infinite domain of integration to a finite region, facilitating the numerical calculations.

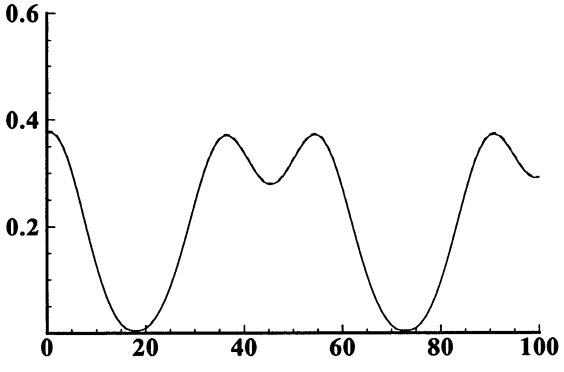

Figure 4. Similar to Fig.3. Gold inclusions in glass.

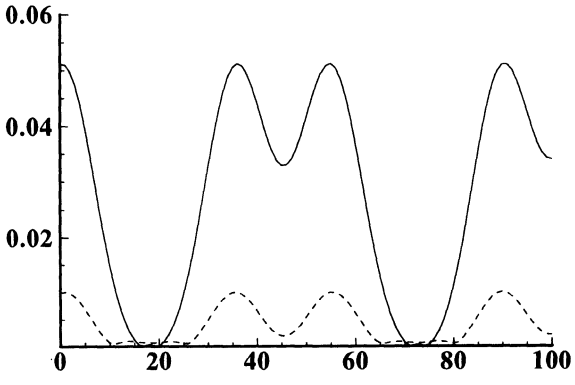

Figure 5. Similar to Fig.3. Yttria inclusions in IN100.

The numerical experiments demonstrate that the change in transmission or reflection represents an approximate image of the interface discriminating the geometry and material contrasts, while Fig. 5 suggests that for weak interfaces reflection images are more satisfactory.

ACKNOWLEDGMENT

JGH was supported by the NSF through grant no. MSS-9114547, and GRW was supported in part by USDOE, contract no. W-7405-ENG-82. We thank F. Margetan, DOE Ames Laboratory, for helpful discussions on the measurement aspects of the work.

REFERENCES

1. J.G. Harris, D.R. Rebinsky and G.R Wickham, J. Acoust. Soc. Am. to appear (1995).
2. F.J. Margetan, R.B. Thompson, J.H. Rose and T.A. Gray, J. Nondestr. Eval. 11, 109 (1992).
3. G.R. Wickham, J. Nondestr. Eval. 11, 199 (1992).
4. E.Yogeswaren and J.G.Harris, J. Acoust. Soc. Am. 96, 3581 (1994).
5. D.A. Rebinsky and J.G. Harris, Proc. Roy. Soc. Lond. A 436, 251 (1992).